Cell, Vol. 109, 335–346, May 3, 2002, Copyright ©2002 by Cell Press

A Senescence Program Controlled by p53 and p16^{INK4a} Contributes to the Outcome of Cancer Therapy

Clemens A. Schmitt,[1,4] Jordan S. Fridman,[1] Meng Yang,[2] Soyoung Lee,[1,4] Eugene Baranov,[2] Robert M. Hoffman,[2] and Scott W. Lowe[1,3]
[1]Cold Spring Harbor Laboratory
1 Bungtown Road
Cold Spring Harbor, New York 11724
[2]AntiCancer, Inc.
7917 Ostrow Street
San Diego, California 92111

Summary

***p53* and *INK4a/ARF* mutations promote tumorigenesis and drug resistance, in part, by disabling apoptosis. We show that primary murine lymphomas also respond to chemotherapy by engaging a senescence program controlled by p53 and p16^{INK4a}. Hence, tumors with *p53* or *INK4a/ARF* mutations—but not those lacking *ARF* alone—respond poorly to cyclophosphamide therapy in vivo. Moreover, tumors harboring a Bcl2-mediated apoptotic block undergo a drug-induced cytostasis involving the accumulation of p53, p16^{INK4a}, and senescence markers, and typically acquire *p53* or *INK4a* mutations upon progression to a terminal stage. Finally, mice bearing tumors capable of drug-induced senescence have a much better prognosis following chemotherapy than those harboring tumors with senescence defects. Therefore, cellular senescence contributes to treatment outcome in vivo.**

Introduction

Chemotherapy remains the primary treatment for systemic malignancies. However, some tumors are inherently insensitive to chemotherapeutic agents and others acquire resistance upon relapse. Most conventional agents damage cellular components, often DNA, and for years it was assumed that this damage was directly responsible for their anti-tumor effect (Johnstone et al., 2002). Consequently, drug resistance was thought to arise primarily from changes that prevented the drug-target interaction, including overexpression of drug efflux pumps (e.g., P-glycoprotein) or intracellular detoxifiers (e.g., glutathione). It is now clear that drug-induced damage is not invariably lethal, but can instead initiate a series of post-damage responses including apoptosis, cell-cycle checkpoints, mitotic catastrophe, and cellular senescence (Chang et al., 1999; Johnstone et al., 2002). Accordingly, the integrity of these damage responses might also influence treatment sensitivity.

Apoptosis is a well-characterized post-damage program that contributes to drug action (Johnstone et al., 2002). Diverse anticancer agents can induce apoptosis through common pathways and, consequently, mutations that disable these pathways can confer multidrug resistance (Lowe et al., 1993). For example, the Bcl2 oncoprotein is a potent suppressor of apoptosis that can produce multidrug resistance in cultured cells and animal models, and Bcl2 overexpression correlates with poor treatment outcome in some clinical settings (Johnstone et al., 2002). Nevertheless, despite extensive efforts, the overall contribution of apoptotic defects to clinical drug resistance has been difficult to assess.

Many of the genes that control apoptosis during tumor development can also influence treatment sensitivity. For example, the p53 tumor suppressor promotes apoptosis in response to stress-inducing stimuli, and, in turn, p53 inactivation facilitates tumor development (Vogelstein et al., 2000). Anticancer agents also activate p53 to promote apoptosis, and loss of p53 function can promote drug resistance in cultured cells and animal models (e.g., Lowe et al., 1993; Schmitt et al., 1999). Hence, *p53* mutations can simultaneously account for a survival advantage during tumor development and inherent resistance to chemotherapeutic drugs. Of note, p53 can also engage several cell-cycle checkpoints and trigger cellular senescence (Bunz et al., 1998; Chang et al., 1999; Kastan et al., 1991; Suzuki et al., 2001; Waldman et al., 1997), although the extent to which these processes contribute to drug action in vivo is not known.

Like *p53*, the *INK4a/ARF* locus is frequently mutated in human cancers and has been linked to treatment sensitivity. This locus encodes two tumor suppressors—ARF and p16^{INK4a}—that share coding sequence translated in different reading frames (Sherr, 2001a). ARF can activate p53 by interfering with its negative regulator Mdm2. Most studies show that ARF is not induced by DNA damage but can potentiate a DNA damage response (de Stanchina et al., 1998; Kamijo et al., 1999). Instead, ARF is induced by mitogenic oncogenes, perhaps as part of a failsafe mechanism that counters hyperproliferative signals (Sherr, 2001a). By contrast, p16^{INK4a} is a cyclin-dependent kinase inhibitor that promotes cell-cycle arrest via the Rb tumor suppressor pathway. *INK4a* regulation is poorly understood, but its expression increases with the onset of cellular senescence (Alcorta et al., 1996; Hara et al., 1996; Robles and Adami, 1998; Serrano et al., 1997). Mutations affecting both *INK4a* and *ARF* are common in malignant tumors, although disruption of either gene alone promotes tumorigenesis in mice and humans (Ruas and Peters, 1998; Sherr, 2001b). *INK4a/ARF* deletions correlate with poor treatment outcome in patients and in mouse models (Maloney et al., 1999; Schmitt et al., 1999), although the precise contribution of each gene product to treatment sensitivity has not been examined.

The determinants of drug action are typically studied in tumor-derived cell lines treated in culture or as xenografts. Animal models that recapitulate the genetics and pathobiology of human malignancies provide powerful alternatives, since these systems are experimentally tractable yet utilize spontaneous tumors treated at their natural site. *Eμ-myc* transgenic mice overexpress the

[3]Correspondence: lowe@cshl.edu
[4]Present address: Max-Delbrück-Center for Molecular Medicine and Charité/Campus Virchow-Hospital, Department of Hematology/Oncology, Humboldt University, D-13353 Berlin, Germany.

Table 1. Designation of Lymphomas With Defined Genetic Lesions (in bold)

Normal cell genotype[a,b]	Retroviral construct	Infection of established lymphomas[c] (lymphomas develop in the absence of the transduced gene)	Infection of hematopoietic stem cells[c] (lymphomas develop in the presence of the transduced gene)
myc $tsg^{+/+}$	no	**ctrl.**	**ctrl.$_{HSC}$**
	MSCV	**ctrl.-MSCV**	**ctrl.$_{HSC}$-MSCV**
	MSCV-bcl2	**ctrl.bcl2**	**ctrl.$_{HSC}$-bcl2**
	MSCV-C9DN	**ctrl.-C9DN**	**ctrl.$_{HSC}$-C9DN**
myc $tsg^{+/-}$	no	***tsg*$^{+/-}$ or *tsg*-null**	***tsg*$^{+/-}{}_{HSC}$ or *tsg*-null$_{HSC}$**
	MSCV	***tsg*$^{+/-}$-MSCV or *tsg*-null-MSCV**	***tsg*$^{+/-}{}_{HSC}$-MSCV or *tsg*-null$_{HSC}$-MSCV**
	MSCV-bcl2	***tsg*$^{+/-}$-bcl2 or *tsg*-null-bcl2**	***tsg*$^{+/-}{}_{HSC}$-bcl2 or *tsg*-null$_{HSC}$-bcl2**
	MSCV-C9DN	***tsg*$^{+/-}$-C9DN or *tsg*-null-C9DN**	***tsg*$^{+/-}{}_{HSC}$-C9DN or *tsg*-null$_{HSC}$-C9DN**

[a] *tsg* (tumor suppressor gene), such as *p53*, *ARF*, or *INK4a/ARF*.
[b] Lymphomas arising from +/+ cells (no targeted gene deletion) form as "controls" (ctrl.).
[c] Lymphomas arising from +/− cells not preserving a functional wild-type sequence—at the time of tumor establishment or after therapy—are considered "null."

c-myc oncogene in the B-cell lineage (Adams et al., 1985), and the resulting B-cell malignancies resemble human non-Hodgkin's lymphomas. We previously developed methods for rapidly producing *Eμ-myc* lymphomas with compound genetic lesions, as well as strategies for studying treatment responses that parallel clinical trials (Schmitt et al., 1999, 2000b, 2002). As in human cancers, mutations that disrupt *p53* or the *INK4a/ARF* locus compromise therapy in *Eμ-myc* lymphomas (Schmitt et al., 1999). Therefore, using this system, the biologic and genetic determinants of drug action can be studied in a relevant setting, yet in a manner not possible in patients. Here, we use the *Eμ-myc* model to explore the biologic and genetic basis for drug action and drug resistance, and find that a senescence program controlled by p53 and p16^{INK4a} is an important determinant of treatment outcome in vivo.

Results

Nonapoptotic Functions of p53 Contribute to Treatment Outcome

The ability of p53 to induce apoptosis in response to DNA damage is considered an important determinant of drug action. Concordantly, both loss of p53 and overexpression of Bcl2 (which acts downstream of p53 to suppress apoptosis) compromise therapy in *Eμ-myc* lymphomas (Schmitt et al., 1999, 2000b). To compare and contrast the impact of these lesions on treatment sensitivity, we generated a panel of primary lymphomas with defined genetic lesions (Schmitt et al., 2000b). We introduced retroviral vectors expressing green fluorescent protein (GFP) alone (MSCV), or coexpressing Bcl2 and GFP (MSCV-bcl2), into primary *Eμ-myc* lymphomas arising in control (ctrl.) or *p53*$^{+/-}$ animals. Note that lymphomas arising in *p53*$^{+/-}$ mice invariably lose the wild-type *p53* allele and become *p53* null. This procedure produced four lymphoma populations, designated as ctrl.-MSCV, ctrl.-bcl2, *p53* null-MSCV, and *p53* null-bcl2, respectively (Table 1). Retrovirally transduced cells were immediately injected into tail veins of syngeneic recipient mice, where the transplanted GFP-tagged lymphoma cells establish tumors histopathologically indistinguishable from the primary malignancies (Schmitt et al., 1999, 2000b). Thus, recipient animals developed systemic lymphomas in which only malignant cells were fluorescent.

Previous studies have shown that GFP can be visualized in tumor xenografts by whole-body fluorescence imaging (Yang et al., 2000). Here, manifestations of GFP-tagged *Eμ-myc* lymphomas were readily visualized in the lymph nodes (LN), bone, and other organs of recipient mice—precisely matching the anatomical locations predicted from pathological evaluation (Figure 1A). Lymphoma-bearing mice were treated with cyclophosphamide (CTX), an alkylating agent that is used against lymphomas and other malignancies. Ctrl.-MSCV tumors typically responded rapidly to CTX, with no GFP fluorescence detectable by 24 hr or thereafter (Figure 1A). In contrast, *p53* null-MSCV tumors underwent a delayed response, and invariably relapsed (Figure 1A). Remarkably, ctrl.-bcl2-transduced tumors displayed virtually no response to CTX, even though it was administered at the maximum tolerated dose. The initial response of these tumors parallels what has been observed in mouse cohorts (Schmitt et al., 1999, 2000b), and indicates that CTX action engages both p53-dependent and independent apoptotic programs.

Although the ctrl.-bcl2 tumors failed to regress following therapy, they did not progress for extended periods (Figure 1A). This is in marked contrast to *p53* null-MSCV and *p53* null-bcl2 tumors, which progressed rapidly (Figure 1A, and data not shown). To extend these results, we compared the tumor-free survival (i.e., time-to-relapse) and overall survival of CTX-treated mice harboring tumors lacking p53 or overexpressing Bcl2. As expected, both lesions prevented mice from achieving long-lasting remissions (Figure 1B; compare to ctrl.-MSCV). However, mice harboring ctrl.-bcl2 lymphomas lived much longer than mice with *p53* null lymphomas (Figure 1B; $p < 0.0001$, e.g., at 30 days: >75% overall survival for ctrl.-bcl2 versus 0% for both *p53* null groups). Bcl2 did not affect overall survival in the *p53* null group, implying that neither its potential role in delaying cell-cycle entry nor its impact on p53-independent apoptosis alters outcome in this model. Still, unlike the ctrl.-MSCV group, all mice harboring ctrl.-bcl2 lymphomas eventually succumbed to their disease (Figure 1B; $p = 0.0061$; >50% versus 0% overall survival at day 100, respectively). Therefore, the initial response to CTX does not neces-

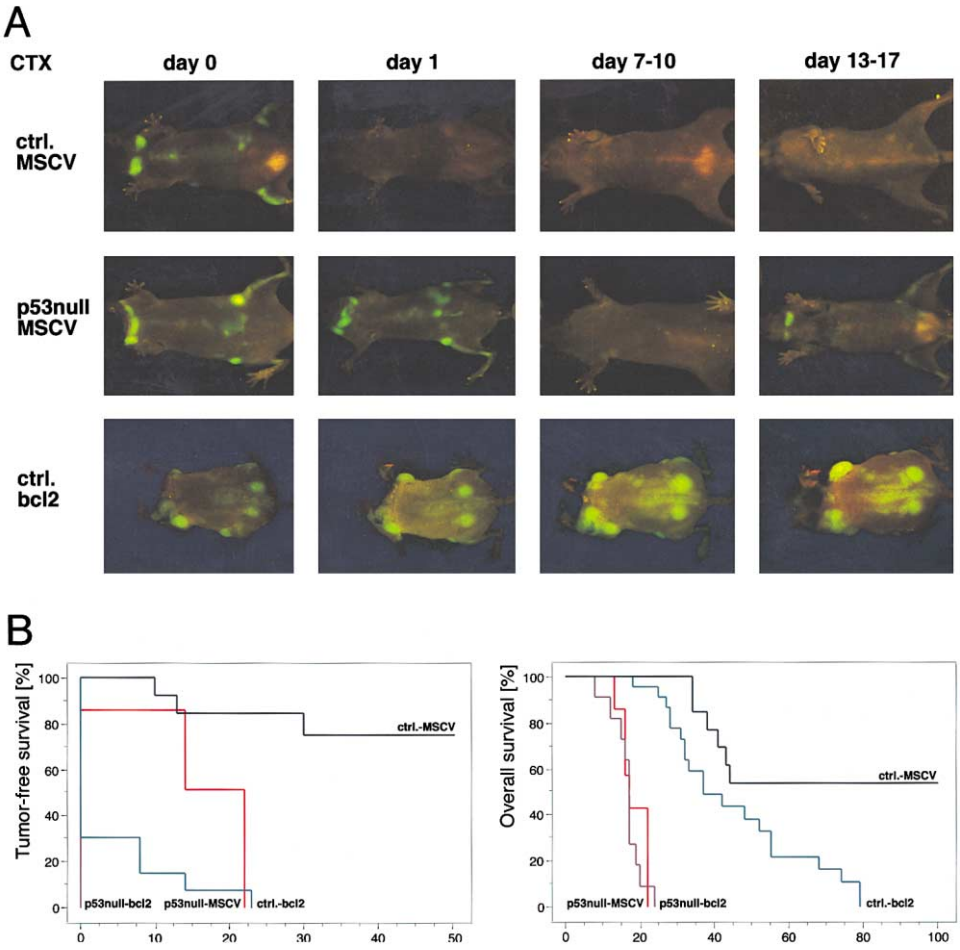

Figure 1. Contribution of p53 and Bcl2 to Treatment Responses

(A) Mice harboring ctrl.-MSCV, *p53* null-MSCV, and ctrl.-bcl2 lymphomas were treated at comparable tumor burdens (day 0) with a single dose of cyclophosphamide (CTX) and monitored by whole-body fluorescence imaging. Representative examples are shown.

(B) Kaplan-Meier plots for tumor-free survival (left) and overall survival (right) following CTX therapy. Curves reflect the response of ctrl.-MSCV (black, n = 13), ctrl.-bcl2 (dark green, n = 23), *p53* null-MSCV (red, n = 7), and *p53* null-bcl2 (purple, n = 11). The mice monitored for disease-free survival are the same as those evaluated for overall survival.

sarily predict treatment outcome. The fact that Bcl2 does not recapitulate the impact of *p53* loss on overall survival implies that nonapoptotic p53 functions are important in treatment sensitivity.

CTX Induces a p53-Dependent Cell-Cycle Arrest In Vivo

The fact that ctrl.-bcl2 tumors remain viable but static for extended periods suggests that CTX can engage a p53-dependent cell-cycle arrest program. Therefore, we measured cell proliferation and p53 expression in CTX-treated lymphomas overexpressing Bcl2. Of note, a subset of lymphomas arising in *Eμ-myc* transgenic mice acquires spontaneous mutations in the p53 pathway, which produces a heterogeneous cohort of ctrl. lymphomas with and without functional p53 (Eischen et al., 1999). To circumvent this problem, MSCV-bcl2-transduced hematopoietic stem cells (HSC; derived from *Eμ-myc* transgenic fetal livers) were used to reconstitute the hematopoietic system of lethally irradiated recipient mice, where they rapidly formed aggressive lymphomas (ctrl.$_{HSC}$-bcl2, Table 1) (Schmitt et al., 2002). Importantly, apoptosis is the only p53 effector function that suppresses *myc*-driven lymphomagenesis, so these Bcl2 expressing lymphomas preserve an intact p53 pathway (Schmitt et al., 2002). Retransplantation of the ctrl.$_{HSC}$-bcl2 lymphomas into several recipients each allowed us to examine the same lymphoma in the presence and absence of CTX therapy. Such tumors are comparable, since the response of the same tumor treated in two different mice is similar (Schmitt and Lowe, 2001).

Upon manifestation of transplanted tumors, LNs were either harvested directly (untreated) or 7 days after CTX treatment. Cell proliferation was estimated by counting mitotic figures, measuring the in vivo incorporation of 5-bromo-2′-deoxyuridine (BrdU), or by staining with the proliferation marker Ki-67. In contrast to untreated lymphomas, CTX-treated tumors completely lacked mitotic figures and were BrdU and Ki67 negative (Figure 2A). Moreover, ctrl.$_{HSC}$-bcl2 tumors displayed sustained in-

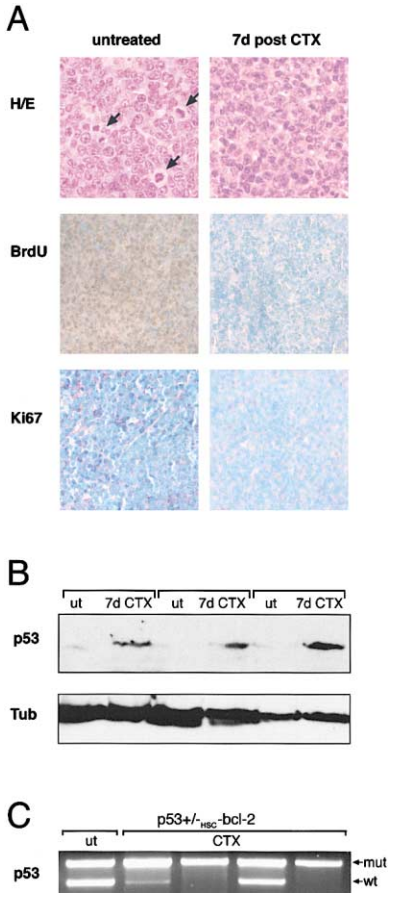

Figure 2. Role of p53 in Drug-Induced Arrest

(A) Ctrl.$_{HSC}$-bcl2 lymphomas were transplanted into several recipients each. Upon tumor formation, parallel tumors originating from the same initial lymphoma were resected from either untreated animals or 7 days post-CTX therapy. Lymph-node sections were stained with hematoxylin-eosin (H/E [top]; high power field; arrows point to mitotic figures) or underwent immunostaining using anti-BrdU or anti-Ki67 antibodies (representative medium power fields are shown).

(B) p53 immunoblot analysis in ctrl.$_{HSC}$-bcl2 lymphomas of samples described in (A). α-Tubulin (Tub) is used as a loading control.

(C) *p53*$^{+/-}_{HSC}$-bcl2 lymphomas were tested for *p53* gene status following two administrations of CTX. The persistence of the mutant (mut) and wild-type (wt) alleles was determined by allele-specific PCR on tumor DNA. Shown are one representative untreated (ut) and 4 CTX-treated samples.

creases in p53 expression post-therapy (Figure 2B). Therefore, CTX is cytostatic to p53-expressing tumors that are insensitive to apoptosis.

If p53 contributes to a prognostically significant arrest program following CTX therapy, then *p53* mutations should confer a selective advantage to tumor cells during therapy, even in the presence of an apoptotic block. Therefore, we introduced MSCV-bcl2 or a dominant-negative *caspase 9* (MSCV-C9DN) into *p53*$^{+/-}$ *Eμ-myc* transgenic fetal liver cells, and allowed lymphomas to form in recipient mice (*p53*$^{+/-}_{HSC}$-bcl2 or *p53*$^{+/-}_{HSC}$-C9DN, respectively). Both genes block apoptosis downstream of p53, and are sufficient to prevent *p53* loss during lymphomagenesis (Schmitt et al., 2002). Consequently, these tumors remained *p53*$^{+/-}$, even upon transplantation into recipient mice (Figure 2C, lane 1, 4/4 tested). However, neither gene prevented *p53* loss during therapy, since most of these lymphomas became *p53* null after two administrations of CTX (2/5 for *p53*$^{+/-}_{HSC}$-bcl2, Figure 2C; 2/2 for *p53*$^{+/-}_{HSC}$-C9DN, data not shown). Concordantly, *p53* null lymphomas—irrespective of their Bcl2 status—did not arrest following CTX therapy (data not shown). Therefore, disruption of a p53-dependent arrest program promotes treatment failure.

Contribution of the *INK4a/ARF* Locus to Tumor Onset and Treatment Outcome

We gained further insights into the determinants of drug action by studying the *INK4a/ARF* locus during tumor development and therapy. Tumors of different genotypes were generated by intercrossing *Eμ-myc* transgenic animals to either *p53*$^{+/-}$, *ARF*$^{+/-}$ mice (targeting exon 1β), or *INK4a/ARF*$^{+/-}$ (targeting exons 2 and 3), all in the C57BL/6 genetic background (see Figure 3A). Consistent with results from mixed backgrounds (Schmitt et al., 1999), tumors arising in each mutant arose with a similar latency yet much more rapidly than controls ($p < 0.0001$, median onset: 32, 34, and 47 days for *p53*$^{+/-}$, *INK4a/ARF*$^{+/-}$, and *ARF*$^{+/-}$ animals, respectively; compare to 139 days for *Eμ-myc* controls; see Supplemental Data available online at http://www.cell.com/cgi/content/full/109/3/335/DC1). Importantly, almost all tumors arising in *p53*$^{+/-}$ and *INK4a/ARF*$^{+/-}$ animals lost the wild-type allele and became *p53* or *INK4a/ARF* null, respectively (Figure 3A and Schmitt et al., 1999). None of the lymphomas arising in the *ARF*$^{+/-}$ background expressed detectable protein (Figure 3A; 17/17 tested, hereafter designated *ARF* null), whereas only ~65% showed loss of exon 1β (*ARF* null$_{Δ1β}$; see also Eischen et al., 1999). Interestingly, Southern blots using an exon-2-specific probe suggested that those *ARF* null tumors in which exon 1β was retained (*ARF* null$_{1β+}$) had heterozygous deletions encompassing exon 2 (Figure 3A, $p = 0.05$). TUNEL analysis of LN sections revealed that *p53* null, *INK4a/ARF* null and *ARF* null lymphomas were less prone to spontaneous apoptosis, suggesting that loss of apoptosis contributed to rapid lymphoma onset (Supplemental Data at above URL). In contrast, disruption of *Rb* or *INK4a* alone had no impact on the onset of *Eμ-myc* lymphomas (Krimpenfort et al., 2001; Schmitt et al., 1999). Consequently, ARF is the sole product of the *INK4a/ARF* locus that suppresses *myc*-induced lymphomagenesis.

INK4a/ARF mutations can compromise therapy in *Eμ-myc* lymphomas (Schmitt et al., 1999). Since loss of *ARF* disables p53 during lymphomagenesis and ARF can potentiate DNA damage responses (de Stanchina et al., 1998; Kamijo et al., 1999; Schmitt et al., 1999), we expected treatment responses of *ARF* null and *INK4a/ARF* null lymphomas to be similar. Lymphomas of the genotypes described above were propagated in syngeneic recipients and treated with CTX upon tumor manifestation. To our surprise, the *ARF* null and *INK4a/ARF* null lymphomas behaved differently: the *ARF* null group responded much better than the *INK4a/ARF* null group (Figure 3B, $p = 0.002$), with tumor-free survival rates

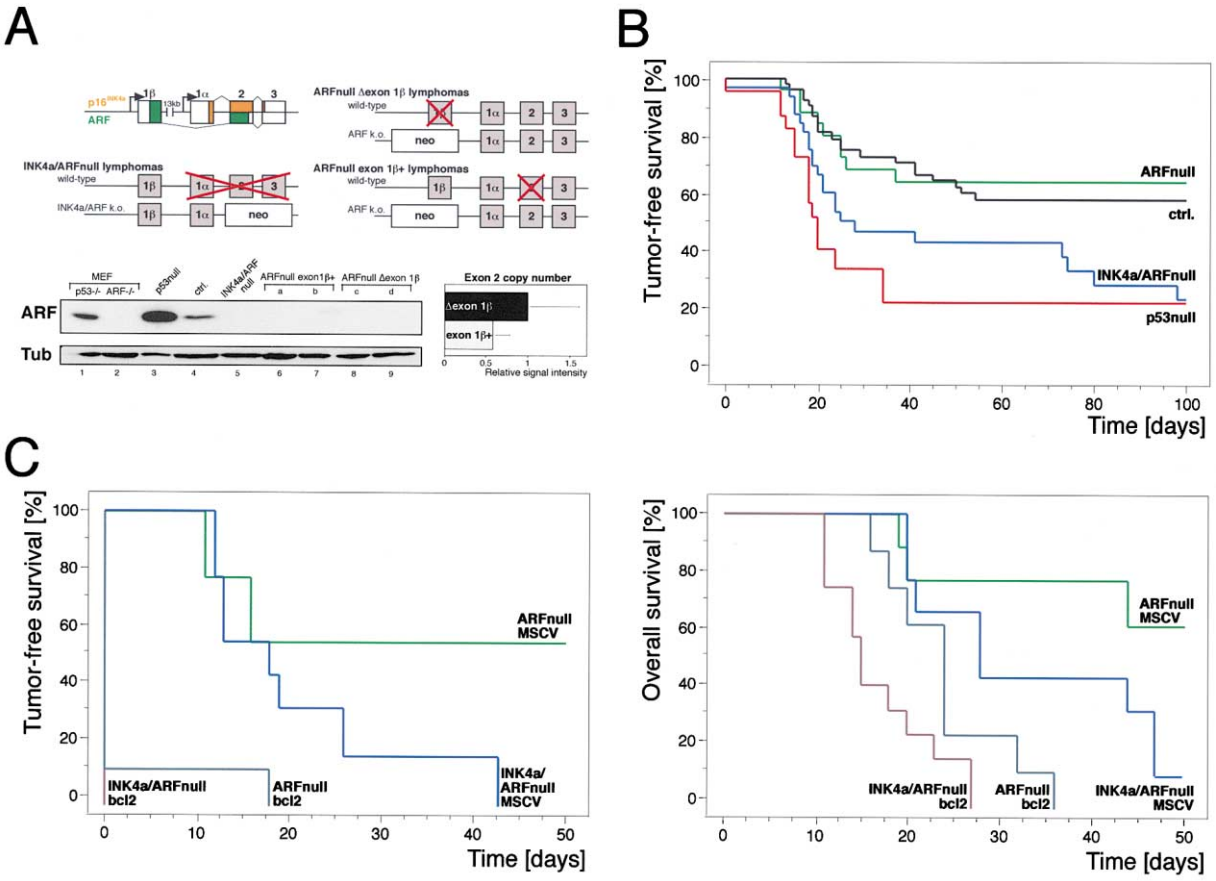

Figure 3. The *INK4a/ARF* Locus in Tumor Development and Treatment Responses

(A) Allelic losses in lymphomas arising in either *INK4a/ARF*$^{+/-}$ or *ARF*$^{+/-}$ genetic backgrounds are illustrated schematically. Greater than 90% of the *INK4a/ARF*$^{+/-}$ derived lymphomas inactivate in >90% both gene products by deletions involving exon 2 (28/31 cases; data not shown). By contrast, only ~65% of *ARF*$^{+/-}$ derived lymphomas (13/20 tested) lost exon 1β (*ARF* null$_{\Delta 1\beta}$; data not shown). Those that retained exon 1β (*ARF* null$_{1\beta+}$, 7/20 tested) may disrupt *ARF* through loss of exon 2 instead, thereby creating *INK4a* heterozygosity. Concordantly, no ARF protein was detected by immunoblotting in any of the *ARF*$^{+/-}$ lymphomas tested (17/17, examples for *ARF* null$_{1\beta+}$ [a, b] and for *ARF* null$_{\Delta 1\beta}$ [c, d] are shown along with *p53*$^{-/-}$ and *INK4a/ARF*$^{-/-}$ MEFs and *p53* null, ctrl., and *INK4a*/ARF null lymphomas for comparison), and Southern blot analysis revealed an almost 50% reduction of exon 2 copy number for *ARF* null$_{1\beta+}$ lymphomas relative to *ARF* null$_{\Delta 1\beta}$ lymphomas (n = 5 each; mean signal intensity ± SD).

(B) Tumor-free survival following CTX treatment of mice harboring ctrl. (black, n = 58), *p53* null (red, n = 24), *ARF* null (green, n = 26) or *INK4a/ARF* null (blue, n = 35) lymphomas. The ctrl., *p53* null, and *INK4a/ARF* null curves incorporate some data previously published (Schmitt et al., 1999).

(C) Tumor-free survival (left) and overall survival (right) in mouse cohorts harboring *ARF* null-MSCV (green, n = 9), *ARF* null-bcl2 (dark green, n = 8), *INK4a/ARF* null-MSCV (blue, n = 9), and *INK4a/ARF* null-bcl2 (purple, n = 12) lymphomas.

similar to those of ctrl. lymphoma bearing mice. Therefore, *INK4a* mutations apparently compromise treatment outcome.

We next examined the impact of *ARF* or *INK4a/ARF* deletions on tumor-free and overall survival following CTX therapy in the presence and absence of Bcl2 (Figure 3C). The overall survival of mice bearing *ARF* null-MSCV tumors was similar to controls (compare to ctrl.-MSCV in Figure 1B), and superior to mice bearing *p53* null-MSCV lymphomas ($p = 0.0025$; compare to Figure 1B). In contrast, mice harboring *INK4/ARF* null-MSCV lymphomas rapidly progressed to a terminal stage ($p = 0.0278$ for overall survival of ctrl.-MSCV [Figure 1B] versus *INK4/ARF* null-MSCV [Figure 3C]). Consequently, the *INK4a/ARF* null group had a much worse prognosis than the *ARF* null group ([Figure 3C], <10% versus >60% surviving at 50 days post-therapy, respectively). Interestingly, whereas Bcl2 had no impact on overall survival in the *p53* null group, it reduced overall survival in the *INK4a/ARF* null setting ($p = 0.0007$). In fact, the overall survival of the *INK4/ARF* null-bcl2 group approached that of both *p53* null groups (Figure 3C; compare to Figure 1B). This suggests that *INK4a* loss and disruption of apoptosis by Bcl2 act independently to promote drug resistance.

Selection Against *INK4a* Genes In Vivo

The above experiments describe how engineered deletions at the *INK4a/ARF* locus affect treatment outcome. Spontaneous mutations also occur at this locus, and their association with poor outcome provides additional evidence that the *INK4a* status influences treatment sen-

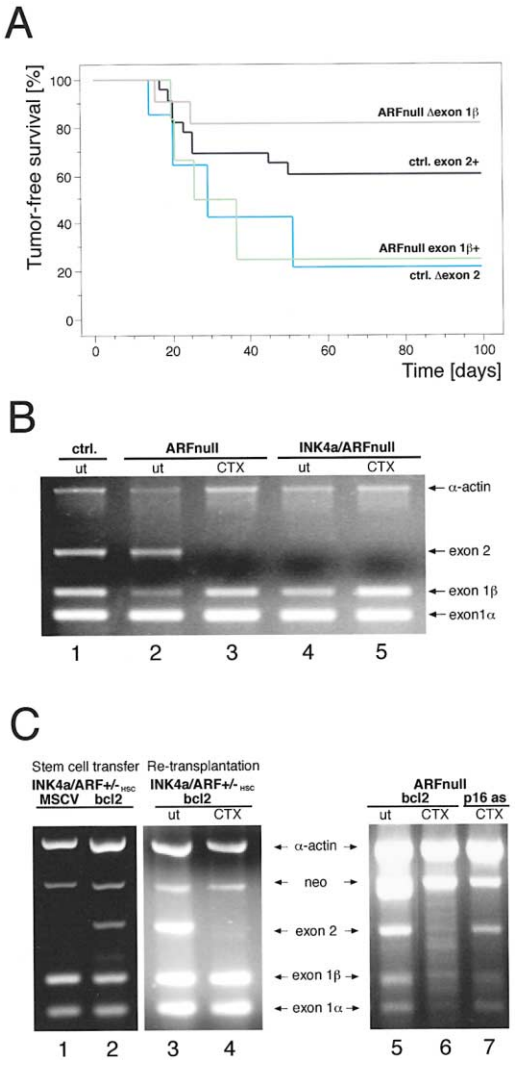

Figure 4. Spontaneous Mutations at the *INK4a/ARF* Locus and Anticancer Therapy

(A) Tumor-free survival for ctrl. and *ARF* null lymphomas after CTX therapy stratified by the *INK4a/ARF* gene status prior to treatment as determined by exon-specific PCR. Compare ctrl. lymphomas with a detectable exon 2 (exon 2^+, black, n = 23) to those with a homozygous deletion in exon 2 (Δexon 2, blue, n = 7). Compare *ARF* $null_{1\beta+}$ lymphomas (light green, n = 6) to *ARF* $null_{\Delta1\beta}$ lymphomas (gray, n = 11).

(B) Multiplex PCR analysis of genomic DNA isolated from the same lymphomas left untreated (ut) or isolated after two rounds of CTX therapy. A representative *ARF* null sample is shown, with a ctrl. and *INK4a/ARF* null sample for comparison. α-actin is a PCR control. Treated *ARF* null lymphomas showed exon 2 deletions in 5 of 7 cases tested.

(C) Left: Primary *INK4a/ARF*$^{+/-}{}_{HSC}$-MSCV and *INK4a/ARF*$^{+/-}{}_{HSC}$-bcl2 lymphomas were isolated and a portion transplanted into syngeneic recipients for subsequent analysis of *INK4a/ARF* status before and after CTX therapy. Shown is a multiplex PCR analysis of genomic DNA from the primary lymphomas or from the transplanted *INK4a/ARF*$^{+/-}{}_{HSC}$-bcl2 lymphomas either left untreated (ut) or following relapse after repeated CTX treatments. α-*actin* and *neomycin* (neo) were included as PCR controls. Right: Aliquots of a primary *ARF* null lymphoma were transduced with either MSCV-bcl2 or MSCV-p16as and transplanted into recipient mice. Shown is a multiplex PCR analysis of genomic DNA isolated from lymphomas left untreated or upon relapse following CTX therapy. A similar result was obtained using another primary *ARF* null lymphoma.

sitivity. For example, *Eμ-myc* lymphomas can acquire homozygous deletions of the *INK4a/ARF* locus (Eischen et al., 1999), and these lesions can be detected by multiplex PCR analysis of genomic DNA using exon-specific primers (see schematic diagram in Figure 3A). Biallelic loss restricted to exon 1α was never observed, and losses restricted to exon 1β (the *ARF* exclusive first exon) were extremely rare (1/52 cases). However, homozygous deletions involving exon 2 were relatively common, occurring in 27% (14/52) of the cases (data not shown). When the CTX response of ctrl. lymphomas was stratified based on their exon 2 status, those with a homozygous deletion of exon 2 responded poorly (p = 0.016), much like the *INK4a/ARF* null group (Figure 4A, compare to 3B).

The response of *ARF* null tumors could be further stratified based on the pretreatment status of exon 1β (Figure 4A). As shown above, *ARF* null lymphomas can arise with (*ARF* $null_{1\beta+}$) or without (*ARF* $null_{\Delta1\beta}$) exon 1β genomic sequences. Remarkably, mice harboring *ARF* $null_{1\beta+}$ tumors responded as poorly as those bearing lymphomas with engineered or spontaneous *INK4a/ARF* deletions (Figure 4A, see also Figure 3B). Moreover, multiplex PCR analysis of lymphoma DNA isolated after two rounds of CTX therapy revealed that the majority had completely lost exon 2 (4 of 6 tested, Figure 4B, compare lane 2 to 3). Therefore, *INK4a* deletions provide a selective advantage to tumor cells during chemotherapy. That most *ARF* $null_{1\beta+}$ lymphomas lost one copy of exon 2 during tumor development may have predisposed these tumors to loss of the other allele during CTX therapy (see Figure 3A).

By contrast, mice harboring *ARF* $null_{\Delta1\beta}$ lymphomas displayed a superb prognosis (p = 0.046, compared to *ARF* $null_{1\beta+}$), even superior to ctrls. (Figure 4A). One explanation for this is that ctrl. lymphomas comprise a heterogeneous group, including subsets acquiring *INK4a/ARF* deletions or *p53* mutations (Eischen et al., 1999; Schmitt et al., 1999) that negatively bias their overall response. However, the *ARF* null group never contained tumors with *p53* mutations (Eischen et al., 1999), and our data imply that those also retaining intact *INK4a* genes are invariably cured by CTX therapy. Indeed, one of the two relapses occurring in the *ARF* $null_{\Delta1\beta}$ subgroup displayed a homozygous deletion encompassing *INK4a* exon 2 (data not shown). Consequently, the majority of the relapses (5/7 tested) in the *ARF* null group could be linked to either a CTX-induced *INK4a* deletion or an *INK4a/ARF* codeletion.

p53 mutations confer an advantage to tumor cells during CTX therapy, even when apoptosis is efficiently blocked (see Figure 2). To determine whether this is also true for the *INK4a/ARF* mutations, we transduced *Eμ-myc INK4a/ARF*$^{+/-}$ hematopoietic stem cells with either MSCV or MSCV-bcl2, and allowed lymphomas to form in recipient mice. MSCV-transduced lymphomas lost the wild-type *INK4a/ARF* allele during lymphoma expansion whereas the MSCV-bcl2 transduced lymphomas did not (Figure 4C, compare lanes 1 and 2). This demonstrates that disruption of apoptosis can substitute for *INK4a/ARF* loss during lymphomagenesis, and provides additional evidence that the cell-cycle inhibitor $p16^{INK4a}$ does not contribute to tumor suppression in this setting (Krimpenfort et al., 2001). *INK4a/ARF*$^{+/-}{}_{HSC}$-bcl2 cells were

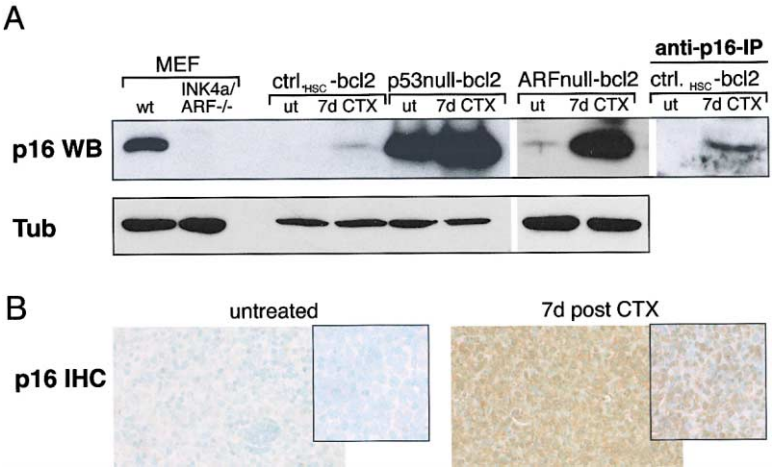

Figure 5. p16^{INK4a} Expression in CTX-Treated Lymphomas Overexpressing Bcl2

(A) Ctrl.$_{HSC}$-bcl2 lymphomas were retransplanted into several recipients and harvested either untreated (ut) or seven days after CTX therapy (7d CTX; as in Figure 2). p16^{INK4a} protein was detected by immunoblotting. *p53* null-bcl2 and *ARF* null-bcl2 samples are shown for comparison, and wild-type (wt), *INK4a/ARF*$^{-/-}$ MEF serve as controls. Shown is a short exposure to visualize p16^{INK4a} inducibility in *p53*-deficient cells (left). Expression of tubulin (Tub) is shown as a loading control. Note that the *ARF* null-bcl2 samples are not the same blot or exposure as the ctrl$_{HSC}$-bcl2 lymphomas. In a different ctrl.$_{HSC}$-bcl2 lymphoma pair, p16^{INK4a} protein levels were detected by anti-p16^{INK4a} immunoprecipitation (IP) preceding immunoblotting (right).

(B) p16^{INK4a} immunohistochemistry (IHC) in a representative ctrl.$_{HSC}$-bcl2 lymphoma sample generated as in (A), (medium power field; high power inlay shows nuclear reactivity).

then injected into syngeneic recipients, and the lymphoma-bearing mice were either left untreated (ut) or were treated with CTX. Whereas the untreated lymphomas retained exon 2, the CTX-treated tumors did not (Figure 4C, compare lanes 3 and 4). Therefore, the *INK4a/ARF* locus encodes a nonapoptotic activity that contributes to treatment sensitivity.

To further evaluate the impact of *INK4a* status on treatment responses, *ARF* null$_{1\beta+}$ lymphomas were transduced with MSCV-bcl2 or MSCV-p16as, an *INK4a*-exon1α-specific antisense construct that effectively suppresses *INK4a* expression (Carnero et al., 2000) (see Supplemental Data). The transduced cells were transplanted into several recipient animals each, and the resulting lymphomas were either harvested directly or after two rounds of CTX therapy. Multiplex PCR analysis revealed that exon 2 was retained in untreated *ARF* null-bcl2 lymphomas but lost upon relapse (Figure 4C, compare lane 5 to 6). In contrast, exon 2 was retained in *ARF* null tumors expressing MSCV-p16as, even after CTX therapy (lane 7). Taken together, our data demonstrate that mutations targeting *INK4a* produce a selective advantage during therapy, thereby contributing to both intrinsic and acquired drug resistance.

p16^{INK4a} Is Activated Following Drug Treatment In Vivo

The data described above demonstrate that *INK4a* gene status is an important determinant of treatment outcome in vivo. Interestingly, p16^{INK4a} acts strictly to promote cell-cycle arrest (Sherr, 2001a), and its expression increases with delayed kinetics following DNA damage in vitro (Robles and Adami, 1998; Suzuki et al., 2001) To determine whether p16^{INK4a} responds to drug treatment in vivo, p16^{INK4a} levels were examined in transplanted ctrl.$_{HSC}$-bcl2 lymphomas before and after CTX therapy. As was observed for p53 (see Figure 2B), p16^{INK4a} levels increased markedly by 7 days post-treatment. This increase was observed by immunoblotting with or without prior anti-p16^{INK4a} immunoprecipitation (Figure 5A), and by immunohistochemical staining of LN sections (Figure 5B). Importantly, ARF was not required for p16^{INK4a} induction, since CTX also induced p16^{INK4a} in *ARF* null lymphomas expressing Bcl2 (Figure 5A). Paradoxically, p16^{INK4a} levels were extremely high in *p53* null lymphomas overexpressing Bcl2, and these levels further increased in response to CTX (Figure 5A). Thus, p16^{INK4a} is activated in response to CTX where, in the presence of p53, it potentiates treatment sensitivity.

Cooperation between p16^{INK4a} and p53

The fact that *p53* null lymphomas express high p16^{INK4a} levels but proliferate suggests that p53 might contribute to p16^{INK4a} action. To test this directly, we reintroduced cDNAs encoding ARF or p16^{INK4a} (MSCV-ARF and MSCV-p16, respectively) into *INK4a/ARF* null or *p53* null lymphomas by retroviral transduction. The coexpressed GFP was monitored by flow cytometry to identify the fraction of cells expressing ARF or p16^{INK4a} (Figure 6A), and proper protein expression was confirmed by immunoblotting (data not shown). Neither ARF nor p16^{INK4a} could be efficiently expressed in *INK4a/ARF* null lymphomas 48 hr after infection (Figures 6A and 6B). However, consistent with ARF acting upstream of p53, a substantial fraction of *p53* null lymphoma cells expressed MSCV-ARF. Surprisingly, *p53* null cells also tolerated MSCV-p16 expression, suggesting that p53 loss reduces selective pressure to eliminate *INK4a*. The fact that high p16^{INK4a} levels—as occur following CTX treatment—are inhibitory to *INK4a/ARF* null cells but not *p53* null cells places p16^{INK4a} either upstream of p53 or in a parallel pathway.

To further delineate the relationship between p53 and p16^{INK4a} in treatment responses, we asked whether *p53* inactivation would alleviate pressure to mutate *INK4a/ARF* during CTX therapy, and vice versa. Indeed, *p53* null;*INK4a/ARF*$^{+/-}$ lymphomas (generated by intercrossing [Schmitt et al., 1999]) never displayed a treatment-induced loss of the remaining *INK4a/ARF* allele (0/5 tested; Figure 6C). Conversely, *p53* was never mutated in *INK4a/ARF* null lymphomas that received multiple rounds of CTX (0/6 tested). Hence, p53 and p16^{INK4a} co-

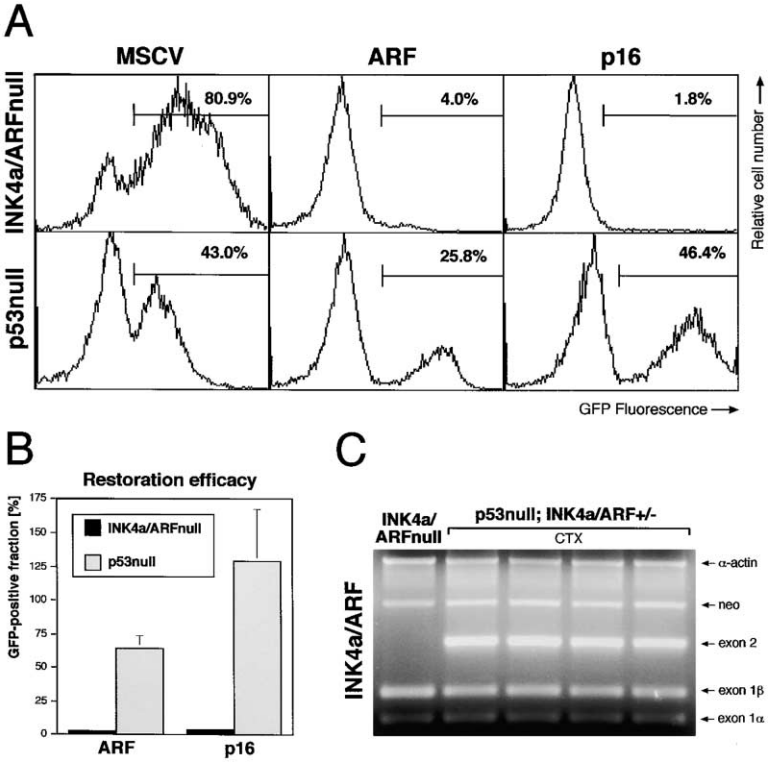

Figure 6. Cooperation Between p16^{INK4a} and p53

(A) Primary lymphomas were infected with MSCV, MSCV-ARF or MSCV-p16 which each co-encode GFP on a bicistronic message, thus allowing measurement of the fraction of infected cells by fluorescence. 48 hr after infection, cells were subjected to flow cytometry to determine the percentage of GFP positive cells.

(B) Quantification of data in (A). Data are plotted relative to the infection efficiency using MSCV (n = 4 for *INK4a/ARF* null and n = 2 for *p53* null lymphomas. Data represent the mean ± SD.

(C) Multiplex PCR analysis of *p53* null;*INK4a/ARF*$^{+/-}$ lymphomas following two rounds of CTX therapy. These lymphomas never lost the remaining *INK4a/ARF* allele (shown are 4/5 cases tested, and an *INK4a/ARF* null lymphoma as a control). Conversely, no *p53* mutations were detected by RT-PCR sequencing in repeatedly CTX-treated *INK4a/ARF* null lymphomas (data not shown).

operate during treatment responses, apparently by engaging a program of prolonged cell-cycle arrest.

Chemotherapy Induces Premature Senescence In Vivo

The cytostasis provoked by CTX is reminiscent of cellular senescence. This program, initially linked to the replicative aging of human fibroblasts in culture (Hayflick and Moorhead, 1961), is considered permanent and is characterized by specific changes including upregulation or the *PML* gene product, and the accumulation of a senescence-associated β-galactosidase (SA-β-gal) activity (Campisi, 2001). Although "replicative" senescence is triggered by telomere malfunction, a similar endpoint can be produced acutely in response to activated oncogenes, oxidative stress, radiation, and certain chemotherapeutic drugs (Chang et al., 1999; Di Leonardo et al., 1994; Serrano et al., 1997). Whether cellular senescence occurs in vivo is controversial, but SA-β-gal-positive cells accumulate in older individuals (Dimri et al., 1995). Most importantly, however, the program is controlled by the p53 and p16/Rb tumor suppressor pathways (Campisi, 2001).

To determine whether CTX-induced cytostasis has features of cellular senescence, we examined SA-β-gal activity in ctrl.$_{HSC}$-bcl2 lymphomas. These lymphomas were chosen because they respond to CTX by a cell-cycle arrest involving p53 and p16^{INK4a} (see above). Individual samples were transplanted into several recipients each, and SA-β-gal activity was examined in lymphoma sections at various times post-treatment. SA-β-gal activity was not detected in untreated lymphomas, but progressively accumulated between 1 and 2 days post-therapy (data not shown), achieving extremely high levels within 7 days (Figure 7A). These tumors also upregulated PML, an independent senescence marker (data not shown). In contrast, *p53* null-bcl2 lymphomas remained negative for SA-β-gal activity. Also, *ARF* null-bcl2 (Figure 5A) accumulated SA-β-gal activity in response to CTX, whereas *INK4a/ARF* null-bcl2 lymphomas did not (Figure 7B). Hence, loss of either *p53* or *INK4a* genes disabled premature senescence provoked by CTX. These findings demonstrate that the outcome of cancer therapy can be linked to a drug-inducible senescence program controlled by p53 and p16^{INK4a}.

Discussion

Cyclophosphamide has been successfully used to treat many human malignancies. Although CTX is not subject to resistance mechanisms involving enhanced drug efflux, many human tumors respond poorly or become resistant to this agent. We used a unique murine lymphoma model to show that the anti-tumor activity of CTX depends on its ability to induce both apoptosis and senescence. Tumors lacking both programs rapidly progress to a lethal stage, suggesting that post-damage responses are almost completely responsible for CTX action. Together, our results establish a paradigm for understanding drug action, as well as the interconnections between tumorigenesis and drug resistance. This paradigm will undoubtedly apply to other conventional anticancer agents, and perhaps many "targeted therapeutics."

Senescence Contributes to Treatment Outcome

Our study provides direct evidence that cellular senescence can be induced following chemotherapy in vivo,

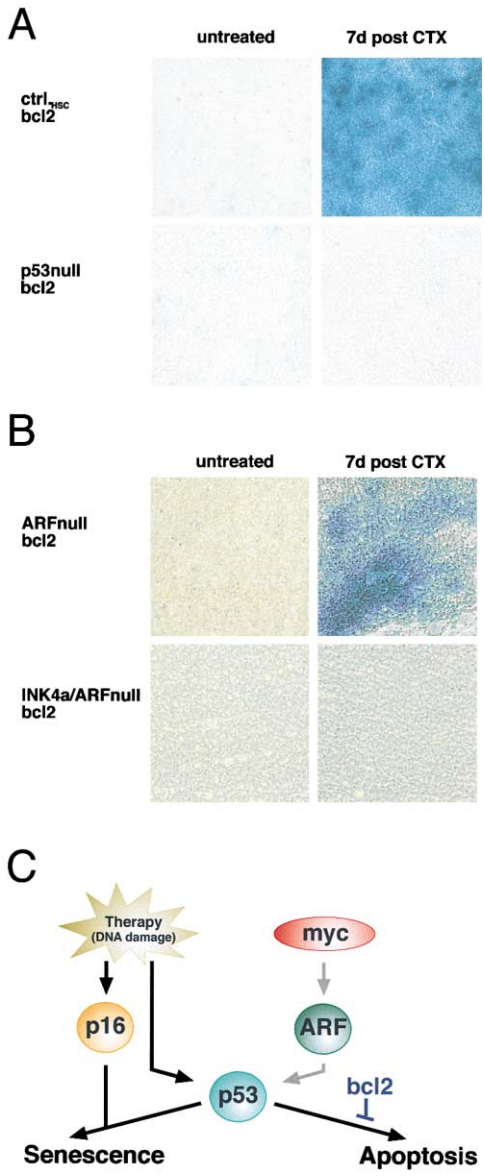

Figure 7. Cellular Senescence and Cancer Therapy In Vivo

(A) Matched pairs (untreated versus seven days post CTX therapy) of ctrl.$_{HSC}$-bcl2 and *p53* null-bcl2 lymphoma sections were compared for senescence-associated β-galactosidase (SA-β-gal) activity in situ (low power field).

(B) Detection of SA-β-gal activity in matched pairs of untreated versus CTX-treated *ARF* null-bcl2 and *INK4/ARF* null-bcl2 lymphomas in situ. As in (A), experiments were conducted at least in duplicate using separate primary lymphomas.

(C) Model of therapy-induced senescence controlled by p16^{INK4a} and p53. CTX, like many other conventional anticancer agents, causes DNA damage which activates p53 through an ARF-independent mechanism. Block of p53-dependent and -independent apoptotic pathways by Bcl2 uncovers senescence as a drug-induced response program. Senescence is disrupted in the context of *p53* or *INK4a/ARF* loss, whereas ARF deficiency alone is not sufficient to disable senescence. p16^{INK4a}, like p53, can be induced by DNA damaging treatment and probably cooperates with p53 in a common arrest program.

leading to an anti-tumor effect. In fibroblasts and epithelial cells, senescence is controlled by the p53 and Rb tumor suppressor pathways, although the contribution of each pathway to the program depends on species and cell type (e.g., Randle et al., 2001). Cell-cycle arrest is considered permanent, and is accompanied by changes in gene expression and upregulation of SA-β-gal activity. Here, drug-induced arrest was accompanied by substantial increases in p53, p16^{INK4a} (an Rb regulator linked exclusively to senescence), PML, and SA-β-gal activity (Figures 2, 5, and 7). Disruption of either *p53* or *INK4a* disabled the arrest program, prevented SA-β-gal accumulation, and acquired loss of either gene often accompanied progression of once dormant tumors to a terminal stage (Figures 2, 5, and 7). The latter observation is consistent with the possibility that CTX-induced cytostasis is stable, and its escape requires rare pre-existing mutations that disable the program. Importantly, the senescence program contributed to treatment outcome, since mice harboring tumors capable of senescence but not apoptosis had a substantially better post-therapy prognosis than those harboring tumors with defects in both processes (Figures 1 and 3).

Cellular senescence may parallel apoptosis as a global response to stress. Indeed, we see that both apoptosis and senescence contribute to drug action, and that loss of either process promotes treatment failure. Interestingly, certain agents that trigger apoptosis in one cell type induce senescence in another, and *p53* and the *INK4a/ARF* locus encode important regulators of both processes. Why some cells undergo apoptosis while others senesce is not known, but we note that drug-induced senescence is most pronounced in the presence of an apoptotic block. This suggests that senescence can serve as a "backup" to apoptosis, and may explain the inability of Bcl2 to enhance clonogenic survival following drug treatment in vitro (Brown and Wouters, 1999). This backup may be particularly important in cell types not naturally prone to apoptosis or in solid cancers that have acquired an apoptotic block during the course of tumor evolution.

p53 Action in Mediating Treatment Responses

Our results clarify the relationship between p53 and treatment sensitivity. Anticancer agents can activate p53 to promote apoptosis, implying that apoptotic defects contribute to the poor outcome of patients harboring *p53* mutant tumors. However, these results do not preclude the possibility that additional p53 activities contribute to drug action. Indeed, ctrl. lymphomas in which apoptosis is disrupted downstream of p53 respond significantly better to therapy than *p53* null tumors (Figure 1). These ctrl.$_{HSC}$-bcl2 tumors do not proliferate and express high p53 levels following therapy; by contrast, *p53* null tumors (irrespective of their Bcl2 status) rapidly progress to a terminal stage. Therefore, the impact of p53 on drug action reflects the combined effects of apoptosis and cellular senescence. Yet other p53 functions may contribute to drug action in some settings (Bearss et al., 2000; Bunz et al., 1999).

Loss of p53 function also accelerates tumorigenesis. We recently demonstrated that apoptosis is the only p53 effector function that suppresses *myc*-induced lym-

phomagenesis (Schmitt et al., 2002). Hence, Bcl2 overexpression in progenitor cells produces lymphomas that are phenotypically identical to *p53* mutant tumors but retain functional p53. Nevertheless, the *p53* mutant tumors, but not those overexpressing Bcl2, display checkpoint defects and aneuploidy, implying that these properties are byproducts of *p53* loss. As shown here, another of these byproducts—defects in cellular senescence—supplies an additional capability to a tumor that is revealed only under therapy. This capability is not conferred to control *Eμ-myc* lymphomas overexpressing Bcl2, despite their equally aggressive pre-treatment behavior. Similarly, *ARF* loss completely disables p53 during lymphomagenesis, yet allows p53 activation during therapy (see Figure 7C). Consequently, *ARF* null tumors respond better to chemotherapy than *p53* null tumors (Figures 1 and 3). Therefore, the precise way in which the p53 pathway is disabled during tumorigenesis can give rise to heterogeneity in treatment responses.

INK4a/ARF Locus and Cancer Therapy

Our data provide the first demonstration that $p16^{INK4a}$ contributes to treatment outcome in vivo, and imply that this reflects its pro-senescence activity. First, tumors with engineered or spontaneous mutations disrupting both *INK4a* and *ARF* are less responsive than those harboring *ARF* mutations alone (Figures 3 and 4). Second, *ARF* null tumors often acquire *INK4a* deletions upon tumor relapse, and antisense *INK4a*-exon 1α can prevent treatment-induced *INK4a* loss (Figure 4). Third, cytostatic tumors retaining *INK4a* and overexpressing Bcl2 display high levels of $p16^{INK4a}$ post-therapy (Figures 5). Finally, *ARF* null tumors retaining *INK4a* have elevated SA-β-gal activity post-therapy while *INK4a/ARF* null tumors do not (Figure 7). Still, while the evidence for $p16^{INK4a}$ involvement in treatment responses is compelling, it does not rule out a role for ARF in some settings (see Supplemental Data available online at http://www.cell.com/cgi/content/full/109/3/335/DC1). As $p16^{INK4a}$ is more strongly associated with senescence in human cells (Sherr and DePinho, 2000), the senescence program it controls may be even more important for drug action in patients.

$p16^{INK4a}$ probably promotes senescence by regulating the Rb pathway. In fact, *Eμ-myc* lymphomas arising in $Rb^{+/-}$ mice respond more poorly than ctrl. lymphomas (C.A.S. and S.W.L., unpublished). However, in *Eμ-myc* lymphomas, $p16^{INK4a}$ action also depends on the presence of wild-type *p53*. *p53* null tumors proliferate despite high levels of endogenous $p16^{INK4a}$, and enforced $p16^{INK4a}$ expression has little anti-proliferative effect (Figures 5 and 6; see also Bardeesy et al., 2001). It is unlikely that $p16^{INK4a}$ induces cell-cycle arrest *through* the p53 pathway; rather, we suspect that these molecules cooperate such that intact p53 function makes the cell permissive for the $p16^{INK4a}$ effect (Figure 7C). Interestingly, p53 initiates, but does not maintain, senescence in murine fibroblasts (Ferbeyre et al., 2002), and it is possible that $p16^{INK4a}$ contributes to the maintenance process.

The way in which the *INK4a/ARF* locus is mutated during tumor development produces heterogeneity in treatment responses. *ARF* mutations promote lymphomagenesis, whereas *INK4a* mutations (alone or in combination with *ARF*) have no additional impact (see Sherr, 2001b and Supplemental Data at above URL). Nevertheless, owing to their proximity, ~25% of *Eμ-myc* lymphomas acquire spontaneous mutations that disable both genes—here, *INK4a* loss is a byproduct of *ARF* mutations. This proximity also allows mutations targeting one gene (*ARF*) during tumor development to facilitate loss of the other gene (*INK4a*) under therapy (Figure 4). Hence, the precise way in which *ARF* is mutated during lymphomagenesis has a profound impact on treatment outcome—mice harboring tumors that have disrupted both genes have a worse prognosis than those with tumors lacking *ARF* alone.

Mouse Models as Test Systems to Study Drug Action

The *Eμ-myc* model provides a unique setting to study drug action (Schmitt et al., 2000a). In this study, we introduced transgenes into hematopoietic stem cells from different genetic backgrounds to rapidly produce tumors with compound genetic lesions, and tagged lymphoma cells with GFP to monitor treatment responses in vivo by fluorescence imaging. These approaches allowed us to dissect the biologic and genetic determinants of drug action in a manner that would be impossible using cell lines or in patients. For example, this system allowed us to spatially and temporally monitor drug responses of individual primary lymphomas in the presence of different genetic lesions, and to study potential gene losses in untreated versus treated mice harboring the same malignancy.

While differences between mice and humans undoubtedly exist, we believe that mouse models have enormous potential for evaluating drug action and predicting treatment responses. Accordingly, much like mice harboring $ctrl._{HSC}$-bcl2 lymphomas, chemotherapy achieves prolonged disease control in patients harboring Bcl2 overexpressing follicular lymphomas, yet these patients eventually enter a progressive clinical course that is associated with acquired *p53* or *INK4a/ARF* mutations (Elenitoba-Johnson et al., 1998; Sander et al., 1993). Similarly, *INK4a* lesions correlate with relapses in Non-Hodgkin's lymphomas that lacked *INK4a* abnormalities at diagnosis (Maloney et al., 1999).

Links between Cancer Genetics and Cancer Therapy

The fact that anticancer agents can rely on pathways that naturally suppress tumorigenesis provides a link between cancer genetics and cancer therapy (Johnstone et al., 2002). For example, apoptosis reveals a brake against tumor development and contributes to the action of anticancer agents; hence, disruption of apoptosis during tumor development can simultaneously select for drug resistant cells (Schmitt et al., 1999). This observation provides one explanation for intrinsic drug resistance—i.e., resistance with no preceding drug exposure. In this study, we identify an unexpected twist to this relationship. We see that byproducts of tumor development—i.e., genetic changes not selected for during tumor evolution—can give rise to acquired capabilities that become relevant only under therapy. This may be because the different components of the tumor

suppressor network play distinct roles during tumor development and therapy (e.g., p53), or because the physical arrangement of certain genes increases the probability that some mutations occur together (e.g., *INK4a/ARF* locus). In either case, this gives rise to heterogeneity in treatment responses that ultimately translate into different prognoses.

The *Eμ-myc* model is remarkably simple. Each tumor analyzed was initiated by the same oncogene (*myc*), arose in the same strain (C57BL/6), and was treated with the same drug (CTX). Yet, these tumors displayed an extraordinary heterogeneity in treatment responses, ranging from cure to progression under therapy depending on their genotype. Given the complexities of human oncology, it is no wonder that treatment responses are remarkably variable and difficult to predict. Undoubtedly this inherent variability will remain a problem, even as we enter the age of targeted therapeutics. Still, our study provides a new paradigm to understand drug action and inherent variations in treatment sensitivity, and provides support for the view that tumor genotype is the most important determinant of treatment outcome. These principles, when applied to human tumors, provide a strong rationale for individualized cancer therapy based on knowledge of drug action and tumor genotype.

Experimental Procedures

Generation of Genetically Defined Lymphomas

Lymphomas harboring loss-of-function lesions were produced by intercrossing *Eμ-myc* transgenic mice with *p53*$^{+/-}$, *ARF*$^{+/-}$ (Δexon1β), or *INK4a/ARF*$^{+/-}$ (Δexon2/3) mice, all in the C57BL/6 background. Genotype and tumor onset were monitored as described (Schmitt et al., 1999). Lymphomas were resected from tumor-bearing mice and either snap frozen, formalin fixed, or processed to single cell suspensions and transplanted into syngeneic recipient mice (Schmitt et al., 1999), or placed in short-term culture for retroviral infection. Introduction of dominant activities into established lymphomas or *Eμ-myc*-derived HSC was conducted as described in detail elsewhere (Schmitt et al., 2000b, 2002). Infected lymphomas or HSC were immediately transplanted into normal or lethally irradiated syngenic recipients, respectively, and lymphoma formation was monitored. All retroviruses were MSCV-IRES-GFP-based vectors (MSCV) containing murine cDNAs such as *bcl2* (MSCV-bcl2), *p16*^{INK4a} (MSCV-p16), *ARF* (MSCV-ARF), the cDNA of a murine dominant-negative *caspase 9* (MSCV-C9DN) (Schmitt et al., 2002), and a *p16*^{INK4a}-exon 1α antisense fragment (MSCV-p16as) (Carnero et al., 2000).

Monitoring Treatment Responses In Vivo

Individual lymphomas were propagated in one or two recipient animals each and treated with a single dose of either cyclophosphamide (CTX [Sigma], 300 mg/kg body weight intraperitoneally) or total body γ-irradiation (6 Gy) when LN enlargements reached about 5 mm (longest diameter, "well-palpable"). Trials examining treatment responses of "matched pairs" are based on identical aliquots of individual primary lymphomas transduced with different transgenes (Schmitt and Lowe, 2001). "Tumor-free survival" was measured as the time between treatment (if achieving a remission within 6 days) and relapse, which is defined as recurrence of a well-palpable LN enlargement within 100 days after therapy (Schmitt et al., 2000a). "Overall survival" reflects the time between treatment and unexpected death or a terminal disease stage. Statistical comparison of Kaplan-Meier curves is based on the log-rank (Mantel-Cox) test. In some animals, fluorescence-based whole-body imaging was used to monitor treatment responses of GFP-tagged lymphomas (Schmitt et al., 2002; Yang et al., 2000).

Monitoring Treatment Responses In Situ and Ex Vivo

Measurement of apoptosis in situ and ex vivo was as described (Schmitt et al., 1999). For analysis of cell proliferation in vivo, primary lymphomas were retransplanted into several animals each. Upon lymphoma formation, one tumor-bearing animal was left untreated while the others received CTX, and the tumors were resected 7 days later. In some cases, 5-bromo-2′-deoxyuridine (BrdU, 100 mg/kg supplemented with 5-fluoro-2′-deoxyuridine) was intraperitoneally administered 6 hr before lymphomas were harvested. BrdU was subsequently detected in paraffin-embedded 7 μm sections using an anti-BrdU antibody (Amersham Pharmacia Biotech). Ki-67 and BrdU were detected by immunohistochemistry using specific antibodies (anti-Ki67 [Dianova, Germany], 1:50 dilution; ImmunoCruz anti-p16^{INK4a} system, Santa Cruz). SA-β-gal activity was assessed as described (Dimri et al., 1995) in 12 μm cryosections derived from treated and untreated animals. Staining was for 12–16 hr at 37°C.

Immunoblotting and Immunoprecipitations

Immunoblotting was carried out using antibodies directed against p53 (CM5, Novocastra, 1:2000 dilution), Bcl2 (13456E, PharMingen, 1:750), ARF (NB200-106, Novus, 1:1000), p16^{INK4a} (M-156, Santa Cruz, 1:500), and α-Tubulin (B-5-1-2, Sigma, 1:2000) as a loading control (Schmitt et al., 1999). For p16^{INK4a} immunoprecipitation, 500 μg of protein lysates were incubated with a 1:40 dilution of M-156 at 4°C for 3 hr. Immunoprecipitation/immunoblotting was carried out as described using a 15%-SDS-polyacrylamide gel followed by immunoblotting with M-156 (de Stanchina et al., 1998).

Mutational Analysis

Loss of heterozygosity (LOH) at the *p53* locus was detected by allele-specific PCR (Schmitt et al., 1999). Mutational analysis of the *p53* gene was carried out using RT-PCR products as described (Schmitt et al., 1999). Gross deletions of the *INK4a/ARF* locus were detected by multiplex PCR analysis of genomic DNA using exon-specific primers for exons 1α, 1β, and 2 as well as for neomycin and α-actin as controls. Primer sequences and exact PCR conditions are available upon request. Southern blots were performed using equal aliquots (10 μg) of BamHI-digested lymphoma DNA samples that were separated on a 0.7% agarose gel and blotted onto a nylon membrane. After hybridization with a ^{32}P-labeled exon 2 probe, specific signals were scanned and quantified using NIH image 1.61 software.

Acknowledgments

We thank A. Harris, T. Jacks, M. Serrano, and C.J. Sherr for mice; K. Sokol for histopathology; L. Bianco, the CSHL animal facility, H. Cosel-Peiper, and C. Rosenthal for technical assistance; G. Ferbeyre for technical advice; and M. McCurrach for editorial advice. We particularly thank E. Querido for providing PML data. This work was supported by a generous gift from the Ann L. and Herbert J. Siegel Philanthropic Fund, a Special Fellowship from the Leukemia and Lymphoma Society (C.A.S.), an NCI training grant and a grant from the Lauri Strauss Leukemia Foundation (J.S.F.), and grants CA89779 (R.M.H.) and CA87497 (S.W.L.) from the National Cancer Institute. S.W.L. is a Rita Allen Scholar.

Received: February 11, 2002
Revised: April 1, 2002

References

Adams, J.M., Harris, A.W., Pinkert, C.A., Corcoran, L.M., Alexander, W.S., Cory, S., Palmiter, R.D., and Brinster, R.L. (1985). The c-myc oncogene driven by immunoglobulin enhancers induces lymphoid malignancy in transgenic mice. Nature *318*, 533–538.

Alcorta, D.A., Xiong, Y., Phelps, D., Hannon, G., Beach, D., and Barrett, J.C. (1996). Involvement of the cyclin-dependent kinase inhibitor p16INK4a in replicative senescence of normal human fibroblasts. Proc. Natl. Acad. Sci. USA *93*, 13742–13747.

Bardeesy, N., Bastian, B.C., Hezel, A., Pinkel, D., DePinho, R.A., and Chin, L. (2001). Dual inactivation of RB and p53 pathways in RAS-induced melanomas. Mol. Cell. Biol. *21*, 2144–2153.

Bearss, D.J., Subler, M.A., Hundley, J.E., Troyer, D.A., Salinas, R.A., and Windle, J.J. (2000). Genetic determinants of response to chemotherapy in transgenic mouse mammary and salivary tumors. Oncogene *19*, 1114–1122.

Brown, J.M., and Wouters, B.G. (1999). Apoptosis, p53, and tumor cell sensitivity to anticancer agents. Cancer Res. *59*, 1391–1399.

Bunz, F., Dutriaux, A., Lengauer, C., Waldman, T., Zhou, S., Brown, J.P., Sedivy, J.M., Kinzler, K.W., and Vogelstein, B. (1998). Requirement for p53 and p21 to sustain G2 arrest after DNA damage. Science *282*, 1497–1501.

Bunz, F., Hwang, P.M., Torrance, C., Waldman, T., Zhang, Y., Dillehay, L., Williams, J., Lengauer, C., Kinzler, K.W., and Vogelstein, B. (1999). Disruption of p53 in human cancer cells alters the responses to therapeutic agents. J. Clin. Invest. *104*, 263–269.

Campisi, J. (2001). Cellular senescence as a tumor-suppressor mechanism. Trends Cell Biol. *11*, S27–31.

Carnero, A., Hudson, J.D., Price, C.M., and Beach, D.H. (2000). p16INK4A and p19ARF act in overlapping pathways in cellular immortalization. Nat. Cell Biol. *2*, 148–155.

Chang, B.D., Broude, E.V., Dokmanovic, M., Zhu, H., Ruth, A., Xuan, Y., Kandel, E.S., Lausch, E., Christov, K., and Roninson, I.B. (1999). A senescence-like phenotype distinguishes tumor cells that undergo terminal proliferation arrest after exposure to anticancer agents. Cancer Res. *59*, 3761–3767.

de Stanchina, E., McCurrach, M.E., Zindy, F., Shieh, S.Y., Ferbeyre, G., Samuelson, A.V., Prives, C., Roussel, M.F., Sherr, C.J., and Lowe, S.W. (1998). E1A signaling to p53 involves the p19(ARF) tumor suppressor. Genes Dev. *12*, 2434–2442.

Di Leonardo, A., Linke, S.P., Clarkin, K., and Wahl, G.M. (1994). DNA damage triggers a prolonged p53-dependent G1 arrest and long-term induction of Cip1 in normal human fibroblasts. Genes Dev. *8*, 2540–2551.

Dimri, G.P., Lee, X., Basile, G., Acosta, M., Scott, G., Roskelley, C., Medrano, E.E., Linskens, M., Rubelj, I., Pereira-Smith, O., et al. (1995). A biomarker that identifies senescent human cells in culture and in aging skin in vivo. Proc. Natl. Acad. Sci. USA *92*, 9363–9367.

Eischen, C.M., Weber, J.D., Roussel, M.F., Sherr, C.J., and Cleveland, J.L. (1999). Disruption of the ARF-Mdm2-p53 tumor suppressor pathway in Myc-induced lymphomagenesis. Genes Dev. *13*, 2658–2669.

Elenitoba-Johnson, K.S., Gascoyne, R.D., Lim, M.S., Chhanabai, M., Jaffe, E.S., and Raffeld, M. (1998). Homozygous deletions at chromosome 9p21 involving p16 and p15 are associated with histologic progression in follicle center lymphoma. Blood *91*, 4677–4685.

Ferbeyre, G., de Stanchina, E., Querido, E., McCurrach, M.E., Hannon, G., and Lowe, S.W. (2002). Oncogenic ras and p53 cooperate to induce cellular senescence. Mol. Cell. Biol., in press.

Hara, E., Smith, R., Parry, D., Tahara, H., Stone, S., and Peters, G. (1996). Regulation of p16CDKN2 expression and its implications for cell immortalization and senescence. Mol. Cell. Biol. *16*, 859–867.

Hayflick, L., and Moorhead, P.S. (1961). The limited in vitro lifetime of human diploid cell strains. Exp. Cell Res. *25*, 585–621.

Johnstone, R.W., Ruefli, A.A., and Lowe, S.W. (2002). Apoptosis: a link between cancer genetics and chemotherapy. Cell *108*, 153–164.

Kamijo, T., van de Kamp, E., Chong, M.J., Zindy, F., Diehl, J.A., Sherr, C.J., and McKinnon, P.J. (1999). Loss of the ARF tumor suppressor reverses premature replicative arrest but not radiation hypersensitivity arising from disabled atm function. Cancer Res. *59*, 2464–2469.

Kastan, M.B., Onyekwere, O., Sidransky, D., Vogelstein, B., and Craig, R.W. (1991). Participation of p53 protein in the cellular response to DNA damage. Cancer Res. *51*, 6304–6311.

Krimpenfort, P., Quon, K.C., Mooi, W.J., Loonstra, A., and Berns, A. (2001). Loss of p16Ink4a confers susceptibility to metastatic melanoma in mice. Nature *413*, 83–86.

Lowe, S.W., Ruley, H.E., Jacks, T., and Housman, D.E. (1993). p53-dependent apoptosis modulates the cytotoxicity of anticancer agents. Cell *74*, 957–967.

Maloney, K.W., McGavran, L., Odom, L.F., and Hunger, S.P. (1999). Acquisition of p16(INK4A) and p15(INK4B) gene abnormalities between initial diagnosis and relapse in children with acute lymphoblastic leukemia. Blood *93*, 2380–2385.

Randle, D.H., Zindy, F., Sherr, C.J., and Roussel, M.F. (2001). Differential effects of p19Arf and p16Ink4a loss on senescence of murine bone marrow-derived preB cells and macrophages. Proc. Natl. Acad. Sci. USA *31*, 9654–9659.

Robles, S.J., and Adami, G.R. (1998). Agents that cause DNA double strand breaks lead to p16INK4a enrichment and the premature senescence of normal fibroblasts. Oncogene *16*, 1113–1123.

Ruas, M., and Peters, G. (1998). The p16INK4a/CDKN2A tumor suppressor and its relatives. Biochim. Biophys. Acta *1378*, F115–177.

Sander, C.A., Yano, T., Clark, H.M., Harris, C., Longo, D.L., Jaffe, E.S., and Raffeld, M. (1993). p53 mutation is associated with progression in follicular lymphomas. Blood *82*, 1994–2004.

Schmitt, C.A., and Lowe, S.W. (2001). Bcl-2 mediates chemoresistance in matched pairs of primary Eμ-myc lymphomas in vivo. Blood Cells Mol. Dis. *27*, 206–216.

Schmitt, C.A., McCurrach, M.E., de Stanchina, E., Wallace-Brodeur, R.R., and Lowe, S.W. (1999). INK4a/ARF mutations accelerate lymphomagenesis and promote chemoresistance by disabling p53. Genes Dev. *13*, 2670–2677.

Schmitt, C.A., Wallace-Brodeur, R.R., Rosenthal, C.T., McCurrach, M.E., and Lowe, S.W. (2000a). DNA damage responses and chemosensitivity in the Eμ-myc mouse lymphoma model. Cold Spring Harb. Symp. Quant. Biol. *65*, 499–510.

Schmitt, C.A., Rosenthal, C.T., and Lowe, S.W. (2000b). Genetic analysis of chemoresistance in primary murine lymphomas. Nat. Med. *6*, 1029–1035.

Schmitt, C.A., Fridman, J.S., Yang, M., Baranov, E., Hoffman, R.M., and Lowe, S.W. (2002). Dissecting p53 tumor suppressor functions in vivo. Cancer Cell *1*, 289–298.

Serrano, M., Lin, A.W., McCurrach, M.E., Beach, D., and Lowe, S.W. (1997). Oncogenic ras provokes premature cell senescence associated with accumulation of p53 and p16INK4a. Cell *88*, 593–602.

Sherr, C.J. (2001a). The INK4a/ARF network in tumour suppression. Nat. Rev. Mol. Cell. Biol. *2*, 731–737.

Sherr, C.J. (2001b). Parsing Ink4a/Arf. "Pure" p16-Null Mice. Cell *106*, 531–534.

Sherr, C.J., and DePinho, R.A. (2000). Cellular senescence: mitotic clock or culture shock? Cell *102*, 407–410.

Suzuki, K., Mori, I., Nakayama, Y., Miyakoda, M., Kodama, S., and Watanabe, M. (2001). Radiation-induced senescence-like growth arrest requires TP53 function but not telomere shortening. Radiat. Res. *155*, 248–253.

Vogelstein, B., Lane, D., and Levine, A.J. (2000). Surfing the p53 network. Nature *408*, 307–310.

Waldman, T., Zhang, Y., Dillehay, L., Yu, J., Kinzler, K., Vogelstein, B., and Williams, J. (1997). Cell-cycle arrest versus cell death in cancer therapy. Nat. Med. *3*, 1034–1036.

Yang, M., Baranov, E., Jiang, P., Sun, F.X., Li, X.M., Li, L., Hasegawa, S., Bouvet, M., Al-Tuwaijri, M., Chishima, T., et al. (2000). Whole-body optical imaging of green fluorescent protein-expressing tumors and metastases. Proc. Natl. Acad. Sci. USA *97*, 1206–1211.